Supporting Information for "Single-Molecule Excitation-Emission Spectroscopy"

*Erling Thyrhaug[1], Stefan Krause[2], Antonio Perri[3], Giulio Cerullo[3], Dario Polli[3,4], Tom Vosch[2], Jürgen Hauer[1,5]**

[1]: Dynamical Spectroscopy, Department of Chemistry, Technical University Munich, Lichtenbergstrasse 4, 85748 Garching, Germany

[2]: Department of Chemistry, University of Copenhagen, Universitetsparken 5, 2100 Copenhagen, Denmark

[3]: IFN-CNR and Dipartimento di Fisica, Politecnico di Milano, Piazza L. da Vinci 32, 20133 Milano, Italy

[4]: Center for Nano Science and Technology@PoliMi, Istituto Italiano di Tecnologia, Via Giovanni Pascoli 70/3, 20133 Milano, Italy

[5]: Photonics Institute, TU Wien, Gußhausstraße 27-29, 1040 Vienna, Austria.

www.pnas.org/cgi/doi/10.1073/pnas.1808290116

TDI STRUCTURE

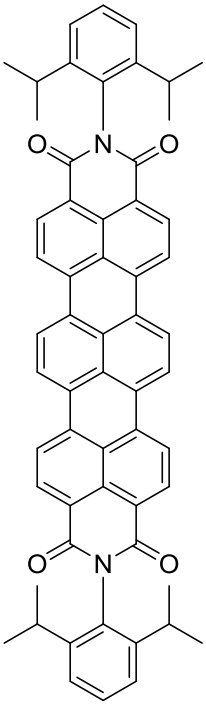

Figure S1: Molecular structure of the terrylene diimide derivative investigated in the Manuscript

COMPARISON OF INTEGRATED BULK SPECTRA

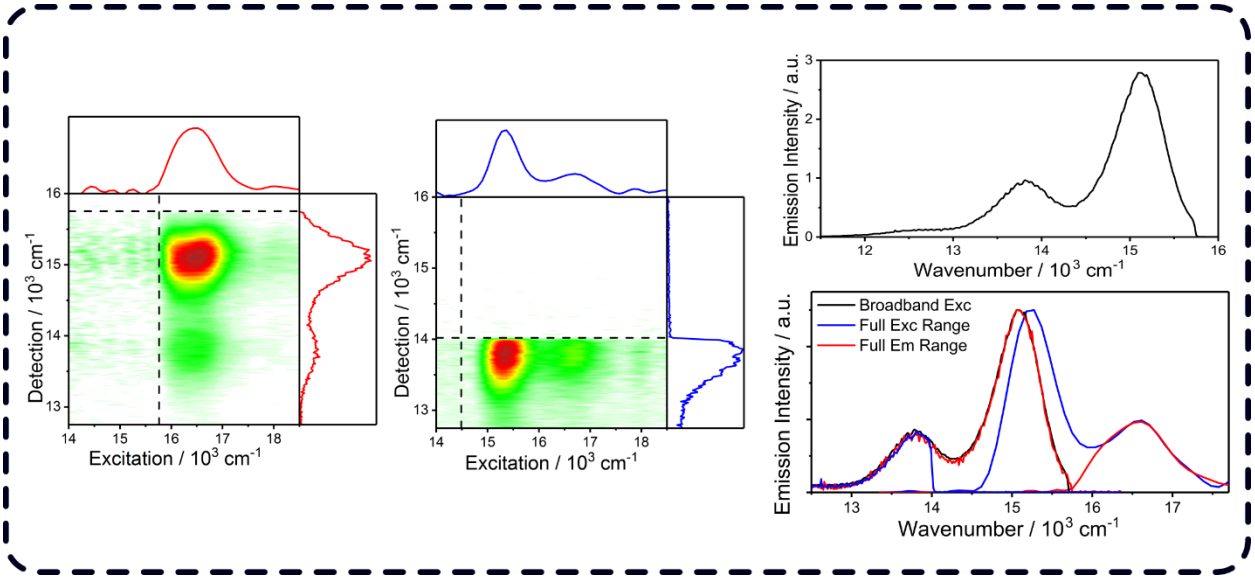

Figure S2: Comparison of bulk TDI spectra. Full emission and excitation range EEMs (left), auxiliary emission spectrum (top right), and an overlay of the integrated spectra (bottom right).

ADDITIONAL SINGLE MOLECULE EEM

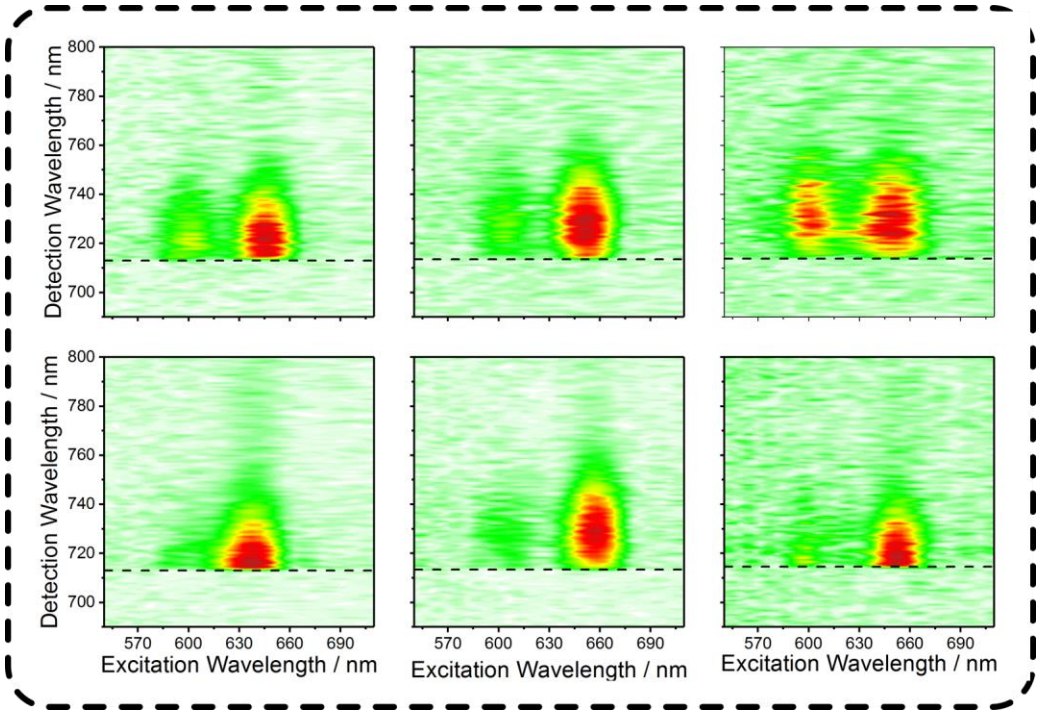

Figure S3: A selection of additional single-molecule EEMs. Filter cut-off indicated by horizontal dashed line

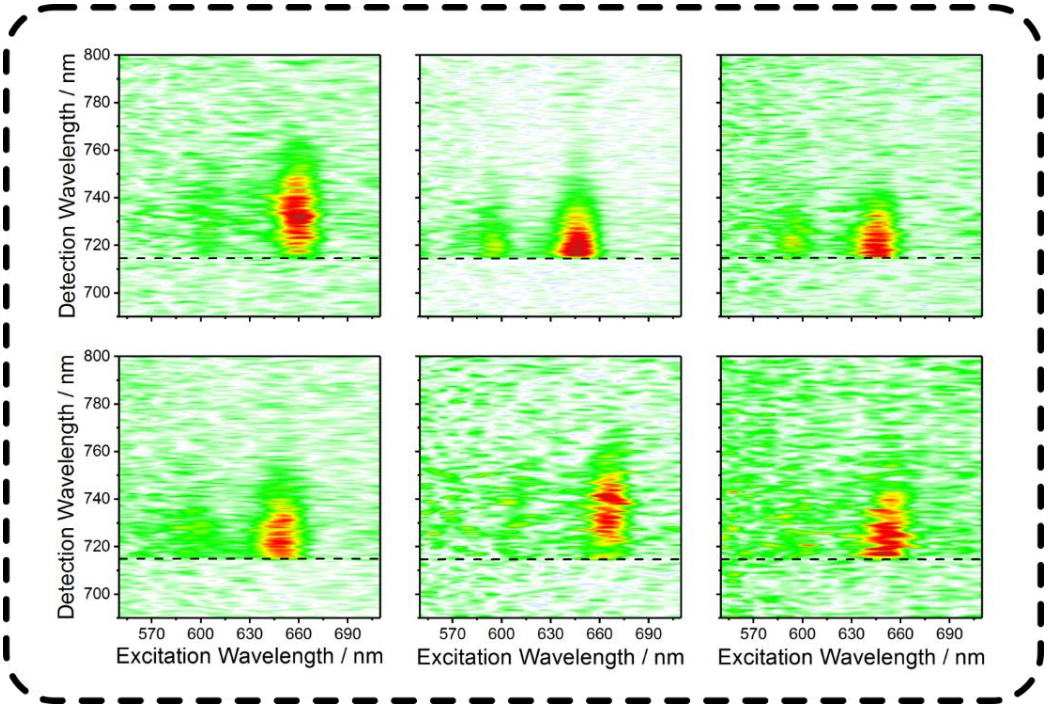

Figure S4: A selection of additional single-molecule EEMs. Filter cut-off indicated by horizontal dashed line

ADDITIONAL EXCITATION WAVELENGTH RESOLVED SMS-TCSPC OF EET DYAD

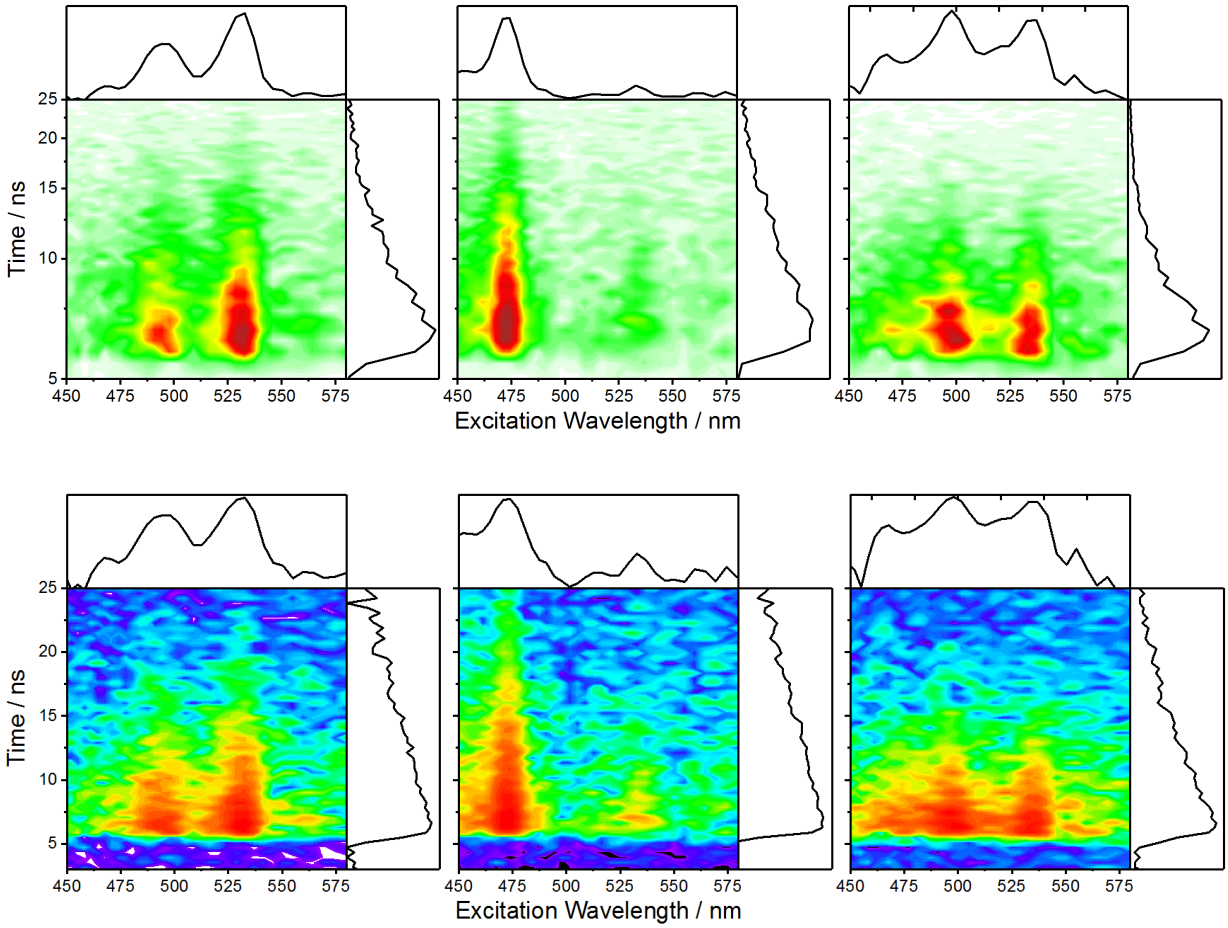

Figure S5: Representative excitation-wavelength resolved TCSPC data of individual EET dyads. Top row: Intensity on linear scale and time axis logarithmic. Bottom row: The same data shown on linear timescale and logarithmic intensity..

DYAD TRANSITION FREQUENCY DISTRIBUTIONS

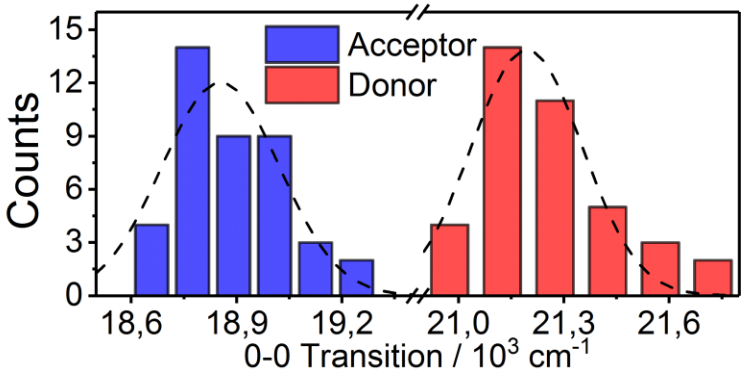

Figure S6: 0-0 transition frequency distribution of donor and acceptor in the EET dyad.

GAUSSIAN FITS TO SMS-EEM LINESHAPES

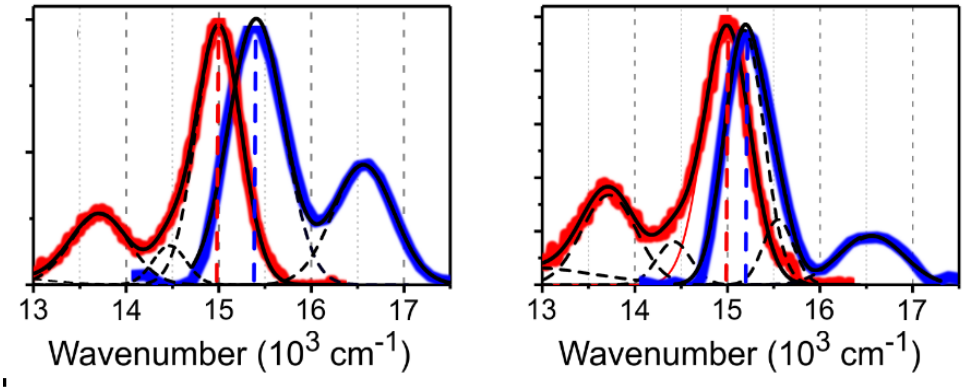

Figure S7: Representative Gaussian fits to the experimental data.

TWINS SPECIFICATIONS

Interferometer: The employed common-path birefringent interferometer is composed by several birefringent optical elements. The entrance and exit polarizers (Pol1 and Pol2 in Figure 1a) are two calcite ($CaCO_3$) Glan-Thompson polarizers with a 1:100,000 extinction ratio over the entire transmission range from 350 nm to 2300 nm. The first birefringent block, namely block A in Figure 1a, is an α-barium borate crystal with 6.3-mm thickness and 10-mm clear aperture. The two identical birefringent wedges of block B are made of the same material of block A with 5.3 mm thickness, 30 mm length and 10º apex angle. The material provides high transmission from 180 nm to 2500 nm with an average birefringence of $\Delta n \approx 0.12$. The maximum achievable delay with this configuration is $\tau = L \tan\alpha \, \Delta n/c \approx 2$ ps, where L is the birefringent wedge length and c is the speed of light in vacuum. This corresponds to ≈0.6 nm resolution at 625-nm wavelength which is however not required in our experiment given the broad linewidth of the dye.

TWINS CALIBRATION PROCEDURE

We report in this section a detailed analytical derivation of the calibration procedure, comparing the working principle of a standard Michelson interferometer with the birefringent interferometer based on the TWINS.

If we consider the usual FT spectroscopy using a Michelson interferometer, the delay τ between the two replicas of a light field $E(\tau)$ does not depend on the wavelength; therefore, one can readily obtain the spectrum $\tilde{S}(\nu)$ as a function of the optical frequency ν as:

$$\tilde{S}(\nu) = \int I(\tau) e^{i2\pi\nu\tau} d\tau$$

where $I(\tau)$ is the interferogram that is given by:

$$I(\tau) = \int \left| \tilde{E}(\nu) + \tilde{E}(\nu) e^{-i2\pi\tau\nu} \right|^2 d\nu$$

Differently, using a birefringent interferometer, the delay τ is wavelength dependent due to the difference between the ordinary and extraordinary refractive indexes, and it is given by: $\tau(\nu, x) = \dfrac{\Delta n(\nu) \cdot \sin\alpha \cdot x}{c}$ where $\Delta n(\nu)$ is the optical frequency-dependent birefringence, x is the wedge insertion, c is the speed of light in the vacuum and α is the wedge apex angle. Therefore, the recorded interferogram as a function of x is given by:

$$I(x) = \int \left| \tilde{E}(\nu) + \tilde{E}(\nu) e^{-i2\pi\tau(\nu,x)\nu} \right|^2 d\nu = \int \left| \tilde{E}(\nu) + \tilde{E}(\nu) e^{-i2\pi \frac{\Delta n(\nu)\cdot\sin\alpha\cdot x}{c}\nu} \right|^2 d\nu$$

From which the spectrum as a function of the spatial frequency f_x can be calculated as:

$$\tilde{S}(f_x) = \int I(x) e^{i2\pi f_x x} dx$$

Since the spatial frequencies depend on the parameters of the device such as the birefringence $\Delta n(\nu)$ and the apex angle α, it is necessary to transform the retrieved entity $\tilde{S}(f_x)$ into $\tilde{S}(\nu)$. To do this we need first of all to find the function $\nu = F(f_x)$ that converts the abscissa values from spatial to optical frequency.

In order to find this relationship we can consider a monochromatic wave with optical frequency $\bar{\nu}$ entering the TWINS interferometer. In this case the recorded interferogram $I(x)$ as a function of the wedge insertion x is a sinusoidal wave, with a spatial period $X = \dfrac{c}{\Delta n(\bar{\nu}) \times \sin\alpha \times \bar{\nu}}$. The Fourier transform of the interferogram $I(x)$ provides a spectrum $\tilde{S}(f_x)$ as a function of spatial frequency f_x, with a peak at $\overline{f_x} = \dfrac{\Delta n(\bar{\nu}) \times \sin\alpha \times \bar{\nu}}{c}$. If one repeats this procedure for a series of monochromatic waves, the result is a curve as a function linking the spatial frequency f_x (vertical axis) and optical frequency v (horizontal axis), such as the one shown in figure S5 . In the same figure we have overlaid the

computed calibration curve $\overline{f_x} = \frac{\Delta n(\bar{\nu}) \times \sin\alpha \times \bar{\nu}}{c}$ employing the well-known Sellmeier equations for the ordinary $n_o(\nu)$ and extraordinary $n_e(\nu)$ refractive indexes of the birefringent material (α-barium borate in our case). The resulting curve (dashed black line) nicely overlaps with the experimental one.

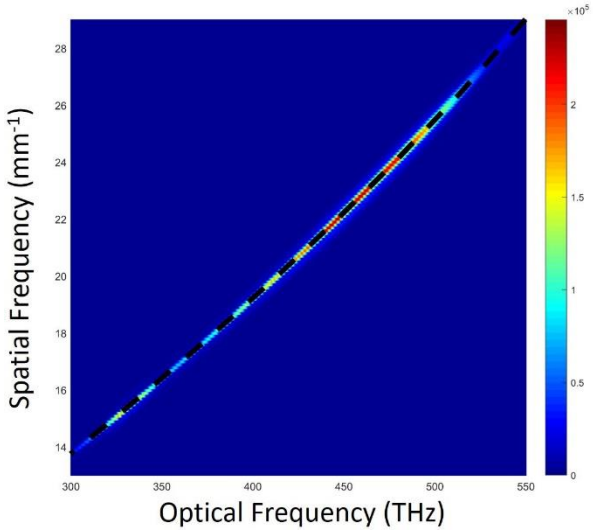

Figure S5: 2D map used for the calibration of the TWINS interferometer and linking the optical frequency to the spatial frequency.

The calibration procedure aims at finding experimentally the function $\nu = F(f_x) = \frac{c \times f_x}{\Delta n(f_x) \times \sin\alpha}$ that maps the specific spatial frequency f_x to the corresponding optical frequency ν. In this way, it is possible to easily convert the spatial frequency axis of the measured spectrum into the optical frequency domain. This can be simply accomplished by using a polynomial fitting from a set of measurements obtained with known optical frequencies. This set of optical frequencies is obtained by using different interferential filters or by using known laser lines or in a more accurate way by measuring the spectral interference at the output of the interferometer with a spectrometer as explained in ref. 24 [Perri *et al.*, "Excitation-emission Fourier-transform spectroscopy based on a birefringent interferometer," Opt. Express 25, A483-A490 (2017)].

After the polynomial interpolation we obtain a set of coefficients P_i such that $\nu = F(f_x) = \sum_1^n P_i f_x^i$ In this way, it is possible to convert the spatial frequencies axis into the corresponding optical frequencies axis, which is device independent. It is important to note that the calibration function is only dependent on the birefringent material and on the wedge apex angle.